Journal of Sound and Vibration (2000) **234**(3), 491–506
doi:10.1006/jsvi.1999.2879, available online at http://www.idealibrary.com on IDEAL®

COMPLEX MODE ACTIVE VIBRATION CONTROL OF HIGH-SPEED FLEXIBLE LINKAGE MECHANISMS

SHAO CHANGJIAN AND ZHANG XIANMIN

Mechatronic Engineering Department, Shantou University, Shantou 515063, *People's Republic of China*

AND

SHEN YUNWEN

Mechanical Engineering Department, Northwestern Polytechnical University, Xi'an 710072, *People's Republic of China*

(*Received* 21 *April* 1999, *and in final form* 29 *December* 1999)

A methodology for suppressing the elastodynamic response of high-speed flexible linkage mechanisms with piezoelectric elements is developed. The finite element active vibration control model is given by a mixed variational approach with Hamilton's principle. On the basis of complex mode theory, a hybrid independent modal controller is developed, which is composed of state feedback and disturbance feedforward control laws. As an illustrative example, the strategy is used to control the elastic vibration response of a four-bar linkage mechanism. The simulation results show that the vibration is efficiently suppressed.

1. INTRODUCTION

For more than two decades, considerable attention has been paid to the investigation of the dynamic analysis and vibration control of flexible mechanisms in order to achieve high-speed and lightweight machines with accurate performances. Heretofore, there are basically five design philosophies which have been developed to improve the elastodynamic responses. The first involves designing links in the conventional materials with optimization of the cross-sectional geometry of the members [1, 2]. The second one uses additional damping materials to dissipate the vibration energy [3]. The third advocates that the mechanism links should be built of advanced composite materials because of their high damping and high stiffness-to-weight ratio [4]. These three design concepts may be referred to as passive vibration control. The fourth introduces a microprocessor-controlled actuator into the original mechanism to reduce the deflection of the flexible linkages [5, 6]. The last involves the application of smart materials featuring distributed actuators and sensors to the linkage mechanisms to control unwanted vibration. These two kinds of control may be classified as active vibration control. With recent advances in composite technology, smart materials, such as optic fibers, piezoelectric ceramics and polymers, electro-rheological fluids, and shape memory alloys, which can be bonded and embedded in composite laminates and structures, come to play a significant role in the active vibration control [7, 8].

A few attempts have been undertaken towards the application of smart materials to control the elastodynamic vibration of lightweight mechanisms. Sung and Chen attempted to control the elastodynamic response of a four-bar linkage mechanism consisting of rigid crank and coupler links and a flexible follower link using piezoceramic elements as

0022-460X/00/280491 + 16 $35.00/0

actuators and sensors [9]. The authors assumed that the free vibration modes of the flexible follower link were the same as those of a simply supported beam. A theoretical development and numerical simulation were given. Liao and Sung derived the finite element equations of the above mechanism and studied the active vibration control problem both analytically and experimentally [10]. In the work of Choi *et al*., a slider-crank mechanism was investigated, whose connecting rod was flexible and was bonded with two piezoelectric films to its upper and lower surfaces [11]. On the basis of the independent modal control method, Zhang *et al*. studied the active vibration control problem for the flexible mechanisms all of whose members were considered as flexible [12]. Recently, Sannah and Smaili presented an experimental investigation into a four-bar mechanism whose follower and coupler links are flexible and the crank is rigid [13]. However, the state-space matrices of the system were assumed to be constant for the entire motion cycle of the mechanism, which is not the case when the mechanism operates at high speeds.

In this paper, a methodology for actively controlling the vibration response of high-speed flexible linkage mechanisms with bonded piezoelectric elements is presented based on complex mode theory. The first part of this paper presents a mathematical model for the high-speed flexible linkage mechanisms equipped with bonded piezoelectric elements employing a mixed variational approach with Hamilton's principle in conjunction with the finite element formulation. This model includes both the terms coupling the elastic and rigid-body motions and the terms coupling the elastodynamics and piezoelectricity. Secondly, an independent modal controller is developed based on the complex mode theory, which is composed of state feedback and disturbances feedforward control. Finally, a four-bar linkage mechanism with all flexible links is employed as an illustrative example to demonstrate the capability of this proposed methodology. This paper ends with some conclusions and perspectives.

2. MODELLING OF THE SYSTEM

2.1. ELEMENT EQUATIONS

The links in the mechanisms are modelled by connecting a series of beam elements. Figure 1 shows a general beam element before and after deformation, as well as the different components of displacement of a point P in the element. This element is integrated with some piezoelectric actuators and sensors, each of which is composed of two layers symmetrically bonded to the upper and lower surfaces of the beam for the purpose of

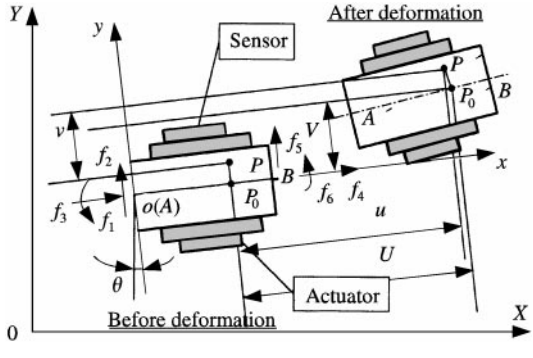

Figure 1. Element displacement field.

simplification of formulation without loss of generality, and perfect bonding is assumed between the connecting surfaces. Here, the Bernoulli beam hypothesis is adopted to describe the displacement of all the components of element. $(O–X–Y)$ is the global fixed frame and $(o–x–y)$ is the local moving frame with $o–x$-axis coincident with the neutral line of the beam element while its original point o is located at its one node before deformation. θ is the angle between these two frames.

Consider a general point $P(x, y)$ in this element. Let P_0 be the correspondent point on the neutral line, and P', P'_0 are their respective positions after deformation. Then the elastic deformation of P_0 is given by

$$U = \sum_i \phi_i(x)u_i \quad (i = 1, 4), \qquad V = \sum_i \phi_i(x)u_i \quad (i = 2, 3, 5, 6), \qquad \varphi = \partial V/\partial x \tag{1}$$

where U and V are the displacements in the x and y directions, respectively, φ is the rotating angle, u_i are the nodal displacements,

$$\{u_1, u_2, u_3, u_4, u_5, u_6\}^{\mathrm{T}} = \{U_A, V_A, \varphi_A, U_B, V_B, \varphi_B\}^{\mathrm{T}}$$

and $\phi_i(x)$ are the shape functions. Since perfect bonding is considered, the deformations of P in all components are uniformly written as

$$u = U - y\frac{\partial V}{\partial x}, \qquad v = V, \qquad \varphi = \frac{\partial V}{\partial x}, \tag{2}$$

where u, v and φ are the displacements in the x and y directions and the rotating angle, respectively. The strains at point P' can be easily determined from the above displacement field:

$$\varepsilon_x = \frac{\partial u}{\partial v} = \frac{\partial U}{\partial x} - y\frac{\partial^2 V}{\partial x^2}. \tag{3}$$

The stresses, however, cannot be expressed in a uniform equation because of the piezoelectricity. In the beam, the stress is

$$\sigma_x = \frac{E(1-\mu)}{(1+\mu)(1-2\mu)}\varepsilon_x, \tag{4a}$$

while in the actuators, according to the linear piezoelectricity [14], the stress is

$$\sigma_x = \frac{E(1-\mu)}{(1+\mu)(1-2\mu)}\varepsilon_x + e_{31}\frac{\Delta v}{h} \tag{4b}$$

and in the sensors,

$$\sigma_x = \left[\frac{E(1-\mu)}{(1+\mu)(1-2\mu)} + \frac{e_{31}^2}{\xi_{33}^{\mathrm{T}} - d_{31}^2 E}\right]\varepsilon_x, \tag{4c}$$

where the E's and μ's are the Young's modulus and the Poisson ratio of the beam, the actuators and the sensors, respectively, Δv is the voltage between the electrodes of actuator, h is the thickness, the e_{31}'s and d_{31} are the stress/charge and strain/charge coefficients, and ξ_{33}^{T} is the free dielectric constant.

The element governing equation of electromechanical behavior can be derived by a variational approach with Hamilton's principle. Hamilton's principle states that the motion of an arbitrary mechanical system occurs in such a way that the definite time integral of the Lagrangian becomes stationary for all the admissible configurations of the

system when the initial (at time t_0) and final (at time t_1) configurations of the system are known [15]. In mathematical terms, this is written as

$$\Delta J = \Delta \int_0^{t_1} (T - W)\,\mathrm{d}t = 0, \tag{5}$$

where T and W are the total kinetic and total potential energies, and Δ represents the variational operator. For the aforementioned element, T is the sum of the kinetic energies of the beam, the actuators, the sensors and the concentrated masses, all referred to the $(O\text{–}X\text{–}Y)$ frame, i.e.,

$$T = T_b + T_a + T_s + T_c, \tag{6}$$

while

$$T_b = \frac{1}{2}\int_{V_b} \rho_b(\dot{X}^2 + \dot{Y}^2)\,\mathrm{d}V,$$

$$T_a = \frac{1}{2}\int_{V_a} \rho_a(\dot{X}^2 + \dot{Y}^2)\,\mathrm{d}V,$$

$$T_s = \frac{1}{2}\int_{V_s} \rho_s(\dot{X}^2 + \dot{Y}^2)\,\mathrm{d}V,$$

where V and ρ represent the volume and the mass density, the subscripts b, a, s and c indicate the beam, the actuators, the sensors and the concentrated masses, respectively, and $(\dot{})$ denotes the time differentiation. Furthermore,

$$X = X_0 + (x + u)c - (y + v)s, \qquad Y = Y_0 + (y + v)c + (x + u)s, \tag{7}$$

where (X_0, Y_0) are the co-ordinates of o in the frame $(O\text{–}X\text{–}Y)$, and $c = \cos\theta$, $s = \sin\theta$. Substituting equations (1)–(2) and equation (7) into equation (6) and writing it in matrix form, we have

$$\begin{aligned} T_b = {} & \tfrac{1}{2}\rho_b A_b L_b(\dot{X}_0^2 + \dot{Y}_0^2) + \tfrac{1}{2}(\rho_b I_b L_b + \tfrac{1}{3}\rho_b A_b L_b^3)\dot{\theta}^2 + \tfrac{1}{2}\rho_b A_b L_b^2\dot{\theta}(\dot{Y}_0 c - \dot{X}_0 s) \\ & + \tfrac{1}{2}\dot{\boldsymbol{\delta}}^{\mathrm{T}}(\mathbf{M}_{1b} + \mathbf{M}_{2b})\dot{\boldsymbol{\delta}} + \tfrac{1}{2}\dot{\theta}^2\boldsymbol{\delta}^{\mathrm{T}}(\mathbf{M}_{1b} + \mathbf{M}_{2b})\boldsymbol{\delta} + \dot{\theta}\dot{\boldsymbol{\delta}}^{\mathrm{T}}\mathbf{b}_b\boldsymbol{\delta} \\ & - \dot{X}_0\dot{\theta}\dot{\boldsymbol{\delta}}^{\mathrm{T}}\mathbf{B}_{1b} + \dot{Y}_0\dot{\theta}\dot{\boldsymbol{\delta}}^{\mathrm{T}}\mathbf{B}_{2b} + \dot{X}_0\dot{\boldsymbol{\delta}}^{\mathrm{T}}\mathbf{B}_{2b} + \dot{Y}_0\dot{\boldsymbol{\delta}}^{\mathrm{T}}\mathbf{B}_{1b} + \dot{\theta}^2\dot{\boldsymbol{\delta}}^{\mathrm{T}}\mathbf{D}_{1b} + \dot{\theta}\dot{\boldsymbol{\delta}}^{\mathrm{T}}(\mathbf{D}_{2b} + \mathbf{D}_{3b}), \end{aligned} \tag{8a}$$

$$\begin{aligned} T_r = {} & \sum_{k=1}^{n_r} \frac{1}{2}\int_{V_r^k} \rho_r^k(\dot{X}^2 + \dot{Y}^2)\,\mathrm{d}V \\ = {} & \sum_{k=1}^{n_r} [\tfrac{1}{2}\rho_r^k A_r^k L_r^k(\dot{X}_0^2 + \dot{Y}_0^2) + \tfrac{1}{2}(\rho_r^k I_r^k L_r^k + \tfrac{1}{3}\rho_r^k A_r^k(x_{2r}^{k^3} - x_{1r}^{k^3}))\dot{\theta}^2 \\ & + \tfrac{1}{2}\rho_r^k I_r^k(x_{2r}^{k^2} - x_{1r}^{k^2})\dot{\theta}(\dot{Y}_0 c - \dot{X}_0 s) \\ & + \tfrac{1}{2}\dot{\boldsymbol{\delta}}^{\mathrm{T}}(\mathbf{M}_{1r}^k + \mathbf{M}_{2r}^k)\dot{\boldsymbol{\delta}} + \tfrac{1}{2}\dot{\theta}^2\boldsymbol{\delta}^{\mathrm{T}}(\mathbf{M}_{1r}^k + \mathbf{M}_{2r}^k)\boldsymbol{\delta} + \dot{\theta}\dot{\boldsymbol{\delta}}^{\mathrm{T}}\mathbf{b}_r^k\boldsymbol{\delta} \\ & - \dot{X}_0\dot{\theta}\dot{\boldsymbol{\delta}}^{\mathrm{T}}\mathbf{B}_{1r}^k + \dot{Y}_0\dot{\theta}\dot{\boldsymbol{\delta}}^{\mathrm{T}}\mathbf{B}_{2r}^k + \dot{X}_0\dot{\boldsymbol{\delta}}^{\mathrm{T}}\mathbf{B}_{2r}^k + \dot{Y}_0\dot{\boldsymbol{\delta}}^{\mathrm{T}}\mathbf{B}_{2r}^k + \dot{\theta}^2\boldsymbol{\delta}^{\mathrm{T}}\mathbf{D}_{1r}^k \\ & + \dot{\theta}\dot{\boldsymbol{\delta}}^{\mathrm{T}}(\mathbf{D}_{2r}^k + \mathbf{D}_{3r}^k)] \quad (r = a \text{ or } s), \end{aligned} \tag{8b}$$

$$T_c = \tfrac{1}{2}(m_L + m_R)(\dot{X}_0^2 + \dot{Y}_0^2) + \tfrac{1}{2}(I_L + I_R + m_R L_b^2)\dot{\theta}^2 + \tfrac{1}{2} m_R L_b \dot{\theta}(\dot{Y}_0 c - \dot{X}_0 s)$$
$$+ \tfrac{1}{2}\dot{\boldsymbol{\delta}}^{\mathrm{T}}(\mathbf{M}_c + \mathbf{M}_1)\dot{\delta} + \tfrac{1}{2}\dot{\theta}^2 \boldsymbol{\delta}^{\mathrm{T}}\mathbf{M}_c\boldsymbol{\delta} + \dot{\theta}\dot{\boldsymbol{\delta}}^{\mathrm{T}}\mathbf{b}_c\boldsymbol{\delta}$$
$$- \dot{X}_0\dot{\theta}\boldsymbol{\delta}^{\mathrm{T}}\mathbf{B}_4 + \dot{Y}_0\dot{\theta}\boldsymbol{\delta}^{\mathrm{T}}\mathbf{B}_3 + \dot{X}_0\dot{\boldsymbol{\delta}}^{\mathrm{T}}\mathbf{B}_3 + \dot{Y}_0\dot{\boldsymbol{\delta}}^{\mathrm{T}}\mathbf{B}_4 + \dot{\theta}^2\boldsymbol{\delta}^{\mathrm{T}}\mathbf{D}_5 + \dot{\theta}\boldsymbol{\delta}^{\mathrm{T}}\mathbf{D}_4, \tag{8c}$$

where $\boldsymbol{\delta}$ and $\dot{\boldsymbol{\delta}}$ are the nodal displacement and velocity vectors,

$$\boldsymbol{\delta} = \{u_1, u_2, \ldots, u_6\}^{\mathrm{T}}, \qquad \dot{\boldsymbol{\delta}} = \{\dot{u}_1, \dot{u}_2, \ldots, \dot{u}_6\}^{\mathrm{T}}.$$

In equation (8), A, I and L are the cross-section area, moment of inertia and length of the components; n_a and n_s are the number of actuators and sensors bonded to the element, m_L, m_R, I_L and I_R are the concerned masses fixed to the left (L) and right (R) ends of the element and their moment of inertia, and the superscript (T) denotes the transpose of matrix.

The potential energy of element is also the sum of those of the beam, the actuators and the sensors, i.e.,

$$W = W_b + W_a + W_s$$
$$= \frac{1}{2}\int_{V_b} \varepsilon_x \sigma_x \,\mathrm{d}V + \frac{1}{2}\sum_{k=1}^{n_0}\int_{V_a^k}\left(\varepsilon_x\sigma_x + \frac{e_{31}^a}{h_a^k}\Delta v_a^k - \frac{\zeta_{33}^{at}}{h_a^{k^2}}\Delta v_a^{k^2}\right)\mathrm{d}V + \frac{1}{2}\sum_{k=1}^{n_s}\int_{V_s^k}\varepsilon_x\sigma_x\,\mathrm{d}V. \tag{9}$$

Substituting equations (1)–(4) into equation (9), through some transformation we get the following matrix form:

$$W = \tfrac{1}{2}\boldsymbol{\delta}^{\mathrm{T}}\left(\mathbf{K}_b + \sum_{k=1}^{n_a}\mathbf{K}_a^k + \sum_{k=1}^{n_s}\mathbf{K}_s^k\right)\boldsymbol{\delta} + \mathbf{v}_a^{e^{\mathrm{T}}}\mathbf{d}_a\,\boldsymbol{\delta} - \tfrac{1}{2}\mathbf{v}_a^{e^{\mathrm{T}}}\mathbf{G}_a\mathbf{v}_a^e, \tag{10}$$

where v_a^e is the vector of input voltage to the actuators

$$\mathbf{v}_a^e = \{\Delta\mathbf{v}_a^1, \Delta\mathbf{v}_a^2, \ldots, \Delta\mathbf{v}_a^{n_a}\}^{\mathrm{T}}.$$

In equation (5), since the rigid-body equations of motion are of no consequence, the variations of X_0, Y_0 and θ are taken to be zero, so the corresponding terms are removed. Generally, the rigid-body motion is assumed to be known previously. Therefore,

$$\Delta J = \Delta\int_{t_0}^{t_1}(T - W)\,\mathrm{d}t = \int_{t_0}^{t_1}\Delta\boldsymbol{\delta}^{\mathrm{T}}\left[\frac{\partial T}{\partial\boldsymbol{\delta}} - \frac{\mathrm{d}}{\mathrm{d}t}\left(\frac{\partial T}{\partial\dot{\boldsymbol{\delta}}}\right) - \frac{\partial W}{\partial\boldsymbol{\delta}}\right]\mathrm{d}t + \int_{t_0}^{t_1}\Delta\mathbf{v}_0^{e^{\mathrm{T}}}\left(-\frac{\partial W}{\partial\mathbf{v}_a}\right)\mathrm{d}t = 0.$$

Furthermore, $\Delta\boldsymbol{\delta}^{\mathrm{T}}$ and $\Delta\mathbf{v}_a^{e^{\mathrm{T}}}$ are independent, so we have

$$\frac{\mathrm{d}}{\mathrm{d}t}\left(\frac{\partial T}{\partial\dot{\boldsymbol{\delta}}}\right) - \frac{\partial T}{\partial\boldsymbol{\delta}} + \frac{\partial W}{\partial\boldsymbol{\delta}} = 0, \tag{11}$$

$$\frac{\partial W}{\partial\mathbf{v}_a^e} = 0. \tag{12}$$

Equation (11) is the Lagrangian equation of element. Incorporating equations (8) and (10) into it yields the equation describing the motion of element being subjected to both mechanical and electric loads and boundary conditions

$$\bar{\mathbf{M}}\ddot{\boldsymbol{\delta}} + \bar{\mathbf{C}}\dot{\boldsymbol{\delta}} + \bar{\mathbf{K}}\boldsymbol{\delta} = \bar{\mathbf{P}} - \mathbf{d}_a^{\mathrm{T}}\mathbf{v}_a^e, \tag{13}$$

where $\bar{\mathbf{M}}$, $\bar{\mathbf{C}}$ and $\bar{\mathbf{K}}$ are the element mass, damping and stiffness matrices, and $\bar{\mathbf{P}}$ is the element load vector. Their expressions are given in Appendix A. From equation (12), we can get the static function equation of actuator

$$\mathbf{d}_a\boldsymbol{\delta} = \mathbf{G}_a\mathbf{v}_a^e. \tag{14}$$

The output voltage of a piezoelectric sensor is given as follows:

$$\Delta\mathbf{v}_s = \frac{1}{C_s}q\,(t) = \frac{1}{C_s}\int_{A_s} e_{31}\varepsilon_x\,\mathrm{d}A,$$

where A_s and C_s are the surface area and capacitance of the sensor, and $q(t)$ is the charge. Considering equation (3), and having the output voltage vector of the element to be

$$\mathbf{v}_s^e = \{\Delta v_s^1, \Delta v_s^2, \ldots, \Delta v_s^{n_s}\}^{\mathrm{T}}$$

we have

$$\mathbf{v}_s^e = \mathbf{d}_s\boldsymbol{\delta}. \tag{15}$$

Therefore, equation (13) and (15) are the equations of motion of the element.

2.2. SYSTEM EQUATIONS

Equations (13) and (15) are in the local co-ordinate system. In order to derive the equations of motion of the global mechanism, they must be transformed to the global co-ordinate system. Let q^e be the nodal displacement vector of an element in the global co-ordinate system (O–X–Y), and define the transformation matrix

$$\mathbf{R} = \begin{bmatrix} c & s & 0 & 0 & 0 & 0 \\ -s & c & 0 & 0 & 0 & 0 \\ 0 & 0 & 1 & 0 & 0 & 0 \\ 0 & 0 & 0 & c & s & 0 \\ 0 & 0 & 0 & -s & c & 0 \\ 0 & 0 & 0 & 0 & 0 & 1 \end{bmatrix}.$$

Then the following equations hold:

$$\boldsymbol{\delta} = \mathbf{R}\mathbf{q}^e, \qquad \dot{\boldsymbol{\delta}} = \dot{\mathbf{R}}\mathbf{q}^e + \mathbf{R}\dot{\mathbf{q}}^e, \qquad \ddot{\boldsymbol{\delta}} = \ddot{\mathbf{R}}\mathbf{q}^e + 2\dot{\mathbf{R}}\dot{\mathbf{q}}^e + \mathbf{R}\ddot{\mathbf{q}}^e. \tag{16}$$

Substituting equation (16) into equations (13) and (15) yields

$$\mathbf{M}^e\ddot{\mathbf{q}}^e + \mathbf{C}^e\dot{\mathbf{q}}^e + \mathbf{K}^e\mathbf{q}^e = \mathbf{P}^e - \mathbf{d}_a^e\mathbf{v}_a^e, \tag{17}$$

$$\mathbf{v}_s^e = \mathbf{d}_s^e\mathbf{q}^e, \tag{18}$$

where

$$\mathbf{M}^e = \mathbf{R}^{\mathrm{T}}\bar{\mathbf{M}}\mathbf{R}, \quad \mathbf{C}^e = \mathbf{R}^{\mathrm{T}}\bar{\mathbf{C}}\mathbf{R} + 2\mathbf{R}^{\mathrm{T}}\bar{\mathbf{M}}\dot{\mathbf{R}}, \quad \mathbf{K}^e = \mathbf{R}^{\mathrm{T}}\bar{\mathbf{K}}\mathbf{R} + \mathbf{R}^{\mathrm{T}}\bar{\mathbf{M}}\ddot{\mathbf{R}} + \mathbf{R}^{\mathrm{T}}\bar{\mathbf{C}}\dot{\mathbf{R}}, \quad \mathbf{P}^e = \mathbf{R}^{\mathrm{T}}\bar{\mathbf{P}},$$

$$\mathbf{d}_a^e = \mathbf{R}^{\mathrm{T}}\mathbf{d}_a, \qquad \mathbf{d}_s^e = \mathrm{d}_s\mathbf{R}.$$

Selecting the vector consisting of all the nodal displacements referred to frame (O–X–Y) to be the generalized displacement vector $\mathbf{q}$ of the linkage system, the vector consisting of all the input voltage of the actuators to be the generalized control vector $\mathbf{v}_a$, and the vector consisting of all the output voltage of the sensors to be the generalized output vector $\mathbf{v}_s$, by assembling all the element equations (17) and (18) with regard to the compatibility at the nodes [16], the equations which describe the motion of flexible linkage mechanism system and the behavior of piezoelectric apparatus are given as

$$\mathbf{M}\ddot{\mathbf{q}} + \mathbf{C}\dot{\mathbf{q}} + \mathbf{K}\mathbf{q} = \mathbf{P} - \mathbf{D}_a\mathbf{v}_a, \tag{19a}$$

$$\mathbf{v}_s = \mathbf{D}_s\mathbf{q}, \tag{19b}$$

where $\mathbf{M}$, $\mathbf{C}$, $\mathbf{K}$, $\mathbf{D}_a$ and $\mathbf{D}_s$ are the systematic mass, damping, stiffness, control and output matrices, respectively, and $\mathbf{P}$ is the systematic generalized force vector.

This model includes both the rigid-body and elastic motion coupling terms [17] and the elastodynamics and piezoelectricity coupling terms, and takes into account the effects of the piezoelectric apparatus upon the mass and the stiffness of the system. Furthermore, it is noted that all the system matrices are not constant but periodically varying functions of the position of each link of the mechanism. However, once the rigid-body motion of system is known, they can be calculated for any position. Therefore, the state-of-the-art method to solve such a kind of periodically varying system is to separate the period of motion into a large number of discrete subintervals in which the system matrices are assumed to be constant. Then, the equations of motion can be solved using some convenient approaches for the systems with constant coefficient matrices.

3. COMPLEX MODE ACTIVE CONTROL OF THE SYSTEM VIBRATION

In the above mathematical model, $\mathbf{C}$ is not composed of the actual structural damping terms but some terms related with the coupling of the elastic and rigid-body motions, and $\mathbf{C}$ and $\mathbf{K}$ are not symmetric matrices, and so cannot be solved using the traditional real mode method. In this section, we develop the method to decouple equation (19) on the basis of complex mode theory. Then we give an independent modal control design approach, which consists of the state feedback and disturbance feedforward control.

3.1. COMPLEX MODE THEORY

Define a state vector x:

$$\mathbf{x} = \{\dot{\mathbf{q}}^{\mathrm{T}}, \mathbf{q}^{\mathrm{T}}\}^{\mathrm{T}}, \qquad \dot{\mathbf{x}} = \{\ddot{\mathbf{q}}^{\mathrm{T}}, \dot{\mathbf{q}}^{\mathrm{T}}\}^{\mathrm{T}}.$$

Rewriting equation (19) in terms of x we obtain

$$\mathbf{A}\dot{\mathbf{x}} + \mathbf{B}\mathbf{x} = \mathbf{Q} + \mathbf{D}\mathbf{v}_a, \qquad \mathbf{v}_s = \mathbf{S}\mathbf{x}, \tag{20a, b}$$

where

$$A = \begin{bmatrix} \mathbf{0} & \mathbf{M} \\ \mathbf{M} & \mathbf{C} \end{bmatrix}, \quad B = \begin{bmatrix} -\mathbf{M} & \mathbf{0} \\ \mathbf{0} & \mathbf{K} \end{bmatrix}, \qquad \mathbf{Q} = \begin{Bmatrix} \mathbf{0} \\ \mathbf{P} \end{Bmatrix}, \qquad \mathbf{D} = -\begin{Bmatrix} \mathbf{0} \\ \mathbf{D}_a \end{Bmatrix}, \qquad \mathbf{S} = [\mathbf{0} \quad \mathbf{D}_s].$$

For equation (20a), we have the generalized eigenvalue problem:

$$\lambda\mathbf{A}\boldsymbol{\chi} + \mathbf{B}\boldsymbol{\chi} = 0, \qquad \lambda\mathbf{A}^{\mathrm{T}}\boldsymbol{\chi}' + \mathbf{B}^{\mathrm{T}}\boldsymbol{\chi}' = 0.$$

Here, because **A** and **B** are not symmetric, their eigenpairs are all complex instead of real. These two equations yield the complex eigenvalues λ_r ($r = 1, 2, \ldots, 2N$, where N is the number of degrees of freedom of the system), the complex left eigenvectors $\boldsymbol{\chi}'_r$ and the complex right eigenvectors $\boldsymbol{\chi}_r$ of the system, which satisfy the orthogonality conditions

$$\boldsymbol{\chi}'^{\mathrm{T}}_r \mathbf{A}\boldsymbol{\chi}_s = \begin{cases} 0 & (r \neq s), \\ a_r & (r = s), \end{cases} \qquad \boldsymbol{\chi}'^{\mathrm{T}}_r \mathbf{B}\boldsymbol{\chi}_s = \begin{cases} 0 & (r \neq s), \\ b_r & (r = s). \end{cases} \tag{21}$$

and $\lambda_r = -b_r/a_r$.

Define the modal matrix

$$\mathbf{X} = [\boldsymbol{\chi}_1 \ \boldsymbol{\chi}_2 \ \cdots \ \boldsymbol{\chi}_{2N}], \qquad \mathbf{X}' = [\boldsymbol{\chi}'_1 \ \boldsymbol{\chi}'_2 \ \cdots \ \boldsymbol{\chi}'_{2N}] \tag{22}$$

and the transformation

$$\mathbf{x} = \mathbf{X}\mathbf{z}. \tag{23}$$

Incorporating equation (23) into equation (20a) and considering the conditions of equations (21) and (22), we have the decoupled system equation

$$\dot{\mathbf{z}} = \boldsymbol{\Lambda}\mathbf{z} + \boldsymbol{\Pi}\mathbf{v}_a + \mathbf{w}, \tag{24}$$

where

$$\boldsymbol{\Lambda} = diag(\lambda_1, \lambda_2, \ldots, \lambda_{2N}), \quad \boldsymbol{\Pi} = [\boldsymbol{\chi}'_1/a_1 \cdots \boldsymbol{\chi}'_{2N}/a_{2N}]^{\mathrm{T}}\mathbf{D} \quad \text{and} \quad \mathbf{w} = [\boldsymbol{\chi}'_1/a_1 \cdots \boldsymbol{\chi}'_{2N}/a_{2N}]^{\mathrm{T}}\mathbf{Q},$$

and z is called the modal co-ordinate vector. The output of the system is transformed to

$$\mathbf{v}_s = \mathrm{SXz} = \mathrm{Hz}. \tag{25}$$

This kind of uncoupled system can be solved independently, so it is much more efficient than when equation (19) is solved directly. All the eigenpairs are seldom required to obtain an accurate solution in practical application. Typically, only the first few modes of vibration are excited within the operating range of the mechanisms. This makes the modal analysis approach extremely suitable for finding the dynamic response of systems with large numbers of degrees of freedom. In the approach developed in this paper, the eigenvalues and eigenvectors are all complex and occur in complex conjugate pairs, so it is called complex mode approach.

3.2. CONTROL DESIGN

Several control synthesis methodologies have been developed in the past years, such as classic PID control, the LQR and LQG techniques robust H_∞ control, etc. [18, 19]. However, their validity in the active control of flexible mechanism vibration needs further investigation. In this study, we develop a simple independent modal space controller, which is composed of an active damper and a feedforward compensator. In this study, all the state variables are supposed to be measurable.

Since it is neither practical nor necessary to control all the vibrational modes of the system with a large number of degrees of freedom because the higher modes do not contribute very much to the solution and therefore need not be taken into account, only the reduced dynamics with the first N_c modes is controlled. The residual dynamics is ensured to be stable by the assumed modal damping. Therefore, the system equation in modal

co-ordinates, equation (24), may be divided into two modal spaces, i.e., the controlled and uncontrolled modal spaces

$$\dot{\mathbf{z}}_c = \mathbf{\Lambda}_c \mathbf{z}_c + \mathbf{\Pi}_c \mathbf{v}_a + \mathbf{w}_c, \qquad \dot{\mathbf{z}}_r = \mathbf{\Lambda}_r \mathbf{z}_r + \mathbf{\Pi}_r \mathbf{v}_a + \mathbf{w}_r, \tag{26}$$

where $\mathbf{z}_c$ contains the first N_c modes, and $\mathbf{z}_r$ is composed of the remaining modes. The matrices $\mathbf{\Lambda}_i$, $\mathbf{\Pi}_i$, and $\mathbf{w}_i$ ($i = c$ and r) are the corresponding system sub-matrices.

System (26) is controllable if and only if $\mathbf{\Pi}_c$ has no rows consisting entirely of zero elements [17]. Assume that the control vector is the sum of two parts

$$\mathbf{v}_a = \mathbf{F}\mathbf{z}_c + \mathbf{v}_2, \tag{27}$$

where the first term, $\mathbf{F}\mathbf{z}_c$, employs the state feedback law to allocate the poles of the system to provide sufficient damping for the controlled modes and $\mathbf{v}_2$ uses the input feedforward law to counteract the generalized force vector $\mathbf{w}_c$, i.e.,

$$\dot{\mathbf{z}}_c = (\mathbf{\Lambda}_c + \mathbf{\Pi}_c F)\mathbf{z}_c + (\mathbf{\Pi}_c \mathbf{v}_2 + \mathbf{w}_c), \qquad \dot{\mathbf{z}}_r = \mathbf{\Pi}_r \mathbf{F}\mathbf{z}_c + \mathbf{\Lambda}_r \mathbf{z}_r + \mathbf{\Pi}_r \mathbf{v}_2 + \mathbf{w}_r. \tag{28}$$

Thus, we set

$$\mathbf{\Pi}_c \mathbf{F} = \mathbf{\Delta\Lambda}_c, \tag{29}$$

where $\mathbf{\Delta\Lambda}_c = diag(\Delta\lambda_1, \ldots, \Delta\lambda_{N_c})$ consists of the differences between the original and required eigenvalues. Premultiply equation (29) with $\mathbf{\Pi}_c^{\mathrm{T}}$,

$$\mathbf{\Pi}_c^{\mathrm{T}} \mathbf{\Pi}_c \mathbf{F} = \mathbf{\Pi}_c^{\mathrm{T}} \mathbf{\Delta\Lambda}_c. \tag{30}$$

This equation yields the state feedback gain matrix $\mathbf{F}$. Furthermore, we set

$$\mathbf{\Pi}_c \mathbf{v}_2 = -\mathbf{w}_c + \mathbf{f}_{re}, \tag{31}$$

where $\mathbf{f}_{re}$ is the reference input. Then $\mathbf{v}_2$ is given by solving the equation

$$\mathbf{\Pi}_c^{\mathrm{T}} \mathbf{\Pi}_c \mathbf{v}_2 = \mathbf{\Pi}_c^{\mathrm{T}}(-\mathbf{w}_c + \mathbf{f}_{re}), \tag{32}$$

$\mathbf{\Delta\Lambda}_c$ and $\mathbf{f}_{re}$ can be optimized with respect to the ability of the actuators and the design requirement.

4. SIMULATION EXAMPLE

In order to demonstrate the validity of the proposed control methodology, a computer simulative analysis is carried out on the four-bar linkage mechanism shown in Figure 2. The property parameters of the mechanism are tabulated in Table 1. There is a concentrated mass 0·2 kg at the joints A and B respectively. A pair of actuators and a pair of sensors are bonded on each of the links. The actuators are manufactured from PZT piezoelectric ceramic with thickness of 0·5 mm, and the sensors from PVDF piezoelectric polymer with thickness of 0·2 mm. The actuator and sensor on the crank link are 30 mm long and 30 mm wide and are located at a quarter and three quarters length of the link while those on the coupler and the follower are 40 mm long and 25 mm wide, and at their three-eighths and five-eighths length. The material properties of the system are given in Table 2.

In this study, all the links are treated as flexible ones. The crank is modelled by two finite elements, and the coupler and follower are both modelled by four elements, so the system has 30 degrees of freedom. The crank speed is 398 r.p.m. The first 5 modes are retained to calculate the response of the system while the first 3 modes are taken as controlled modes,

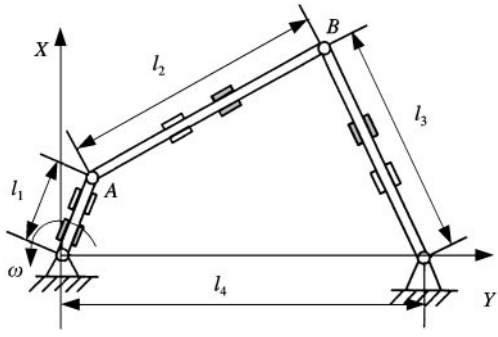

Figure 2. Four-bar mechanism with piezoelectric apparatus. ☐ Sensor. ▭ Actuator.

TABLE 1

Parameters of the mechanism links

Parameters	Link 1	Link 2	Link 3	Link 4
Length (mm)	98·8	302·0	300·0	332·2
Width (mm)	30	25	25	—
Thickness (mm)	5	3	3	—

TABLE 2

The material properties

Properties	Links	Actuators	Sensors
Density ρ (kg/m^3)	2700	7500	1760
Young's modulus E (N/m^2)	7×10^{10}	$1{\cdot}17 \times 10^{11}$	$0{\cdot}15 \times 10^{10}$
The Poisson ratio μ	0·25	0·25	0·25
Dielectric constant ξ_{33}^{T} ($\times 8{\cdot}85 \times 10^{-12}$ F/m)	—	1700	12
Piezoelectric constant d_{31} (m/V)	—	$185{\cdot}0 \times 10^{-12}$	$20{\cdot}0 \times 10^{-12}$

i.e., $N_c = 6$ and $N_r = 4$. In the control synthesis, the controlled modal damping ratios are increased from 0·01 to 0·03, and the reference input is set to be 30% of the generalized modal force.

Figure 3 shows the X and Y direction elastodynamic responses of the midpoint of the coupler link both with and without control. It is seen that a significant vibration suppression is achieved: the responses come to be steady much faster and the steady state responses are remarkably suppressed after employing the control.

In Figure 4, are the plots of the actuator control voltages. It is observed that, at the beginning of the control action, high-voltage magnitudes are required to provide sufficient active damping and the voltages vary violently. When the system comes to be steady, the input voltages exhibit a regular periodicity and their magnitudes are much less, which are mainly composed of the feedforward components. This indicates that a much more

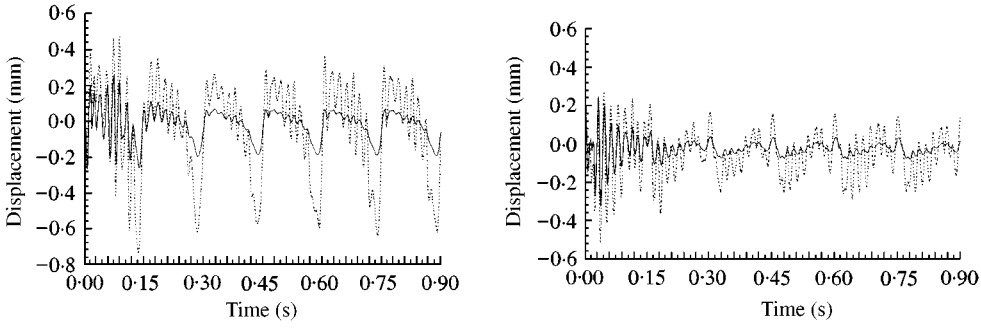

Figure 3. Comparison of the responses with and without control. (a) Response in the X direction. (b) Response in the Y direction. (····) Uncontrolled; (—) Controlled.

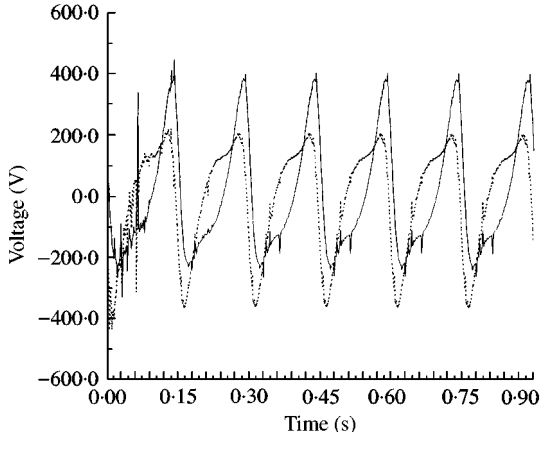

Figure 4. Input voltages of the actuators. (—) Coupler; (·····) Follower.

expensive facility is needed to achieve the efficient active damping for the linkage mechanisms.

A balance between the vibration control level and the control input must be achieved because the practical actuators can only endure limited voltage. The tolerant voltage of the PZT actuator used in this paper is from -500 to $+500$ V, so the control voltage must not exceed this range. Otherwise, the actuator will lose its piezoelectricity and fail to work at all. The results shown in Figures 3 and 4 satisfy such constraints.

During the process of the study, the efficiency of the controller is found to be very sensitive to the variation of the position, configuration and dimension of the actuators and sensors, and the above is the result after some trial-and-error work. We will present the optimization of the actuators and sensors in some subsequent works.

In this paper, the controller is designed to solely improve the dynamic characteristics of the controlled subsystem. When the closed-loop controlled system equation (28) is set-up, however, the effect of the control input upon the residual subsystem cannot be neglected. The effect may deteriorate the control efficiency regarding the whole system because it probably excites violent vibrations of the residual modes if the control is not inputted properly. This is called "spillover". How to overcome this phenomenon is the aim of our further research.

5. CONCLUSIONS

An elastodynamic analysis and control of the high-speed flexible linkage mechanisms incorporated with piezoelectric actuators and sensors has been investigated. A mixed variatioal approach with Hamilton's principle has been developed to derive the finite element equations that describe the motion of the mechanisms and the behavior of the piezoelectric apparatus. This model includes both the rigid-body and elastic motion coupling terms and the elastodynamics and piezoelectricity coupling terms as well as the effects of the actuators and sensors upon the mass and stiffness of the system. An independent modal space control methodology based on the complex mode theory has been proposed. The computer simulation carried out upon a four-bar planar linkage mechanism shows that the vibration is significantly suppressed.

This study demonstrates clearly the validity of the proposed methodology. More researches should be undertaken toward the synthesis of a more efficient controller using some advanced control laws and the optimization of the actuators and sensors. The experimental implementation of the complicated controller also needs further investigation.

ACKNOWLEDGMENT

The research was supported by the National Natural Science Foundation of China under grants 59975056 and 59605001, the Natural Science Foundation of Guangdong Province under grant 970381, and the Foundation of Guangdong Province under grant 9912 to the second author. Their support is gratefully acknowledged.

REFERENCES

1. W. L. Cleghorn, F. G. Fenton and B. Tabarrok 1981 *Mechanism of Machine Theory* **16**, 339–406. Optimal design of high-speed flexible mechanisms.
2. Zhang Xianmin, Shen Yunwwen, Liu Hongzhao and CaoWeiqing 1995 *Mechanism & Machine Theory* **30**, 131–139. Optimal design of flexible mechanisms with frequency constraints.
3. E. H. El-Dannah and S. H. Farghaly 1993 *Mechanism & Machine Theory* **28**, 447–457. Vibratory response of a sandwich link in a high-speed mechanism.
4. A. Ghazavi, F. Gardanine and N. G. Chalhout 1993 *Computers and Structures* **49**, 315–325. Dynamic analysis of a composite material flexible robot arm.
5. J. H. Oliver, D. A. Wysocki and B. S. Thompson 1985 *Mechanical Machine Theory* **20**, 471–482. The synthesis of flexible linkages by balancing the tracer point quasi-static deflections using microprocessor and advanced material technologies.
6. K. Soong, D. Sunappan and B. S. Thompson 1987 *Advanced Topics in Vibrations*, *DE*-Vol. **8**, *The 1987 ASME Design Technology Conference*, *Boston MA*, September 27–30, 147–160. The elastodynamic response of a class of intelligent machinery. Part I: theory. Part II: computational and experimental results.
7. C. K. Lee 1990 *Journal of the Acoustic Society of America* **87**, 1144–1158. Theory of laminated piezoelectric plates for the design of distributed sensors/actuators. Part I: governing equations and reciprocal relationships.
8. C. K. Lee and F. C. Moon 1990 *ASME Journal of Applied Mechanics* **57**, 434–441. Modal sensors/actuators.
9. C. K. Sung and Y. C. Chen 1991 *ASME Journal of Vibration and Acoustics* **113**, 14–21. Vibration control of the elastodynamic response of high-speed flexible linkage mechanisms.
10. C. Y. Liao and C. K. Sung 1993 *ASME Journal of Mechanical Design* **115**, 658–665. An elastodynamic analysis and control of flexible linkages using piezoceramic sensors and actuators.
11. S. B. Choi, C. C. Cheong, B. S. Thompson and M. V. Gandhi 1994 *Mechanism & Machine Theory* **29**, 535–546. Vibration control of flexible linkage mechanisms using piezoelectric films.

12. ZHANG XIANMIN, LIU HONGZHAO AND CAOWEIQING 1996 *Chinese Journal of Mechanical Engineering* **32**, 9–16. Active vibration control of flexible mechanisms.
13. M. SANNAH AND A. SMAILI 1998 *ASME Journal of Mechanical Design* **120**, 316–326. Active control of elastodynamic vibrations of a four-bar mechanism system with a smart coupler link using optimal multivariable control: experimental implementation.
14. K. SUN AND F. X. ZHANG 1984 *The Piezoelectricity* (*Chinese*). Beijing: National Defence Industry Press.
15. F. CHARETTE 1994 *Journal of the Acoustic Society of America* **96**, 2274–2283. Asymmetric actuation and sensing of a beam using piezoelectric materials.
16. A. MIDHA, A. G. ERDMAN AND D. A. FROHRIB 1978 *Mechanism & Machine Theory* **13**, 603–618. Finite element approach to mathematical modeling of high-speed elastic linkages.
17. A. G. JABLOKOW, S. NAGARAJAN AND D. A. TURCIC 1993 *ASME Journal of Mechanical Design* **115**, 314–323. A modal analysis solution technique to the equations of motion for elastic mechanism systems including the rigid-body and elastic motion coupling terms.
18. J. V. DE. VEGTE 1990 *Feedback Control Systems*. Englewood Cliffs, NJ: Prentice-Hall, Inc, Second Edition.
19. A. BAZ AND S. POH 1992 *ASME Journal of Dynamic Systems, Measurement, and Control* **114**, 96–103. Independent modal space control with positive position feedback.

APPENDIX A

In equation (13),

$$\bar{M} = M_{1b} + M_{2b} + M_c + M_I + \sum_{k=1}^{n_a} (M_{1a}^k + M_{2a}^k) + \sum_{k=1}^{n_s} (M_{1s}^k + M_{2s}^k)$$

$$\bar{C} = 2\dot{\theta}\left(b_b + \sum_{k=1}^{n_a} b_s^k + \sum_{k=1}^{n_s} b_s^k + b_c\right),$$

$$\bar{K} = K_b + \sum_{k=1}^{n_a} K_a^k + \sum_{k=1}^{n_s} K_s^k - \dot{\theta}^2\left[M_{1b} + M_{2b} + M_c + \sum_{k=1}^{n_a} (M_{1a}^k + M_{2a}^k) + \sum_{k=1}^{n_s} (M_{1s}^k + M_{2s}^k)\right] + \ddot{\theta}\left(b_b + \sum_{k=1}^{n_a} b_a^k + \sum_{k=1}^{n_s} b_s^k + b_c\right),$$

$$\bar{P} = -\ddot{X}_0\left(B_{2b} + B_3 + \sum_{k=1}^{n_a} B_{2a}^k + \sum_{k=1}^{n_s} B_{2s}^k\right) - \ddot{Y}_0\left(B_{1b} + B_4 + \sum_{k=1}^{n_a} B_{1a}^k + \sum_{k=1}^{n_s} B_{1s}^k\right) + \dot{\theta}^2\left(D_{1b} + D_5 + \sum_{k=1}^{n_a} D_{1a}^k + \sum_{k=1}^{n_s} D_{1s}^k\right) - \ddot{\theta}\left[D_{2b} + D_{3b} + D_4 + \sum_{k=1}^{n_a} (D_{2a}^k + D_{3a}^k) + \sum_{k=1}^{n_s} (D_{2s}^k + D_{3s}^k)\right],$$

$$d_a = [d_{ij}]_{n_a \times 6}$$

$$= \begin{cases} \dfrac{e_{31}^a A_a^i}{h_a^i} \displaystyle\int_{x_{1a}^i}^{x_{2a}^i} \phi_j'(x)\,\mathrm{d}x & \text{(The upper and lower layers of the } i\text{th actuator are polarized in the same direction, and } j = 1, 4.) \\ -\dfrac{e_{31}^a A_a^i}{h_a^{i^2}}(y_{2a}^{i^2} - y_{1a}^{i^2}) \displaystyle\int_{x_{1a}^i}^{x_{2a}^i} \phi_j''(x)\,\mathrm{d}x & \text{(The upper and lower layers of the } i\text{th actuator are polarized in reverse direction, and } j = 2, 3, 5, 6.) \\ 0 & \text{(For other cases.)} \end{cases}$$

and

$$M_{1b} = [m_{ij}]_{6\times 6} = \rho_b A_b \begin{cases} \int_0^{L_b} \phi_i(x)\phi_j(x)\,\mathrm{d}x, & i,j = 1,4, \\ \int_0^{L_b} \phi_i(x)\phi_j(x)\,\mathrm{d}x, & i,j = 2,3,5,6, \\ 0 & \text{for other cases,} \end{cases}$$

$$M_{2b} = [m_{ij}]_{6\times 6} = \rho_b I_b \begin{cases} \int_0^{L_b} \phi_i'(x)\phi_j'(x)\,\mathrm{d}x, & i,j = 2,3,5,6 \\ 0 & \text{for other cases,} \end{cases}$$

$$M_{1r}^k = [m_{ij}]_{6\times 6} = \rho_r^k A_r^k \begin{cases} \int_{x_{1r}^k}^{x_{2r}^k} \phi_i(x)\phi_j(x)\,\mathrm{d}x, & i,j = 1,4, \\ \int_{x_{1r}^k}^{x_{2r}^k} \phi_i(x)\phi_j(x)\,\mathrm{d}x, & i,j = 2,3,5,6, \ (r = a,s) \\ 0 & \text{for other cases,} \end{cases}$$

$$M_{2r}^k = [m_{ij}]_{6\times 6} = \rho_r^k I_r^k \begin{cases} \int_{x_{1r}^k}^{x_{2r}^k} \phi_i'(x)\phi_j'(x)\,\mathrm{d}x, & i,j = 2,3,5,6 \ (r = a,s), \\ 0 & \text{for other cases,} \end{cases}$$

$M_c = diag(m_L, m_L, 0, m_R, m_R, 0)$, $M_L = diag(0, 0, I_L, 0, 0, I_R)$,

$$b = [b_{ij}]_{6\times 6} = \rho_b A_b \begin{cases} -\int_0^{L_b} \phi_i(x)\phi_j(x)\,\mathrm{d}x, & i = 1,4, \ j = 2,3,5,6, \\ \int_0^{L_b} \phi_i(x)\phi_j(x)\,\mathrm{d}x, & i,j = 2,3,5,6, \ j = 1,4, \\ 0 & \text{for other cases,} \end{cases}$$

$$b_r^k = [b_{ij}]_{6\times 6} = \rho_r^k A_r^k \begin{cases} -\int_{x_{1r}^k}^{x_{2r}^k} \phi_i(x)\phi_j(x)\,\mathrm{d}x, & i = 1,4, \ j = 2,3,5,6, \\ \int_{x_{1r}^k}^{x_{2r}^k} \phi_i(x)\phi_j(x)\,\mathrm{d}x, & i = 2,3,5,6, \ j = 1,4 \ (r = a,s), \\ 0 & \text{for other cases,} \end{cases}$$

$$b_c = \begin{bmatrix} 0 & -m_L & 0 & 0 & 0 & 0 \\ m_L & 0 & 0 & 0 & 0 & 0 \\ 0 & 0 & 0 & 0 & 0 & 0 \\ 0 & 0 & 0 & 0 & -m_R & 0 \\ 0 & 0 & 0 & m_R & 0 & 0 \\ 0 & 0 & 0 & 0 & 0 & 0 \end{bmatrix}$$

$$K_b = [k_{ij}]_{6\times 6} = \frac{(1-\mu_b)E_b}{(1+\mu_b)(1-2\mu_b)} \begin{cases} A_b \int_0^{L_b} \phi_i'(x)\phi_j'(x)\,\mathrm{d}x, & i,j = 1,4, \\ I_b \int_0^{L_b} \phi_i''(x)\phi_j''(x)\,\mathrm{d}x, & i,j = 2,3,5,6, \\ 0 & \text{for other cases,} \end{cases}$$

$$K_a^k = [k_{ij}]_{6\times 6} = \frac{(1-\mu_a)E_a}{(1+\mu_a)(1-2\mu_a)} \begin{cases} A_a^k \int_{x_{1a}^k}^{x_{2a}^k} \phi_i'(x)\phi_j'(x)\,\mathrm{d}x, & i,j = 1,4, \\ I_a^k \int_{x_{1a}^k}^{x_{2a}^k} \phi_i''(x)\phi_j''(x)\,\mathrm{d}x, & i,j = 2,3,5,6, \\ 0 & \text{for other cases,} \end{cases}$$

$$K_s^k = [k_{ij}]_{6\times 6}$$

$$= \left[\frac{(1-\mu_s)E_s}{(1+\mu_s)(1-2\mu_s)} + \frac{e_{31}^{s^2}}{\xi_{33}^{\mathrm{T}} - d_{31}^{s^2}E_s}\right] \begin{cases} A_a^k \int_{x_{1s}^k}^{x_{2s}^k} \phi_i'(x)\phi_j'(x)\,\mathrm{d}x, & i,j = 1,4, \\ I_s^k \int_{x_{1s}^k}^{x_{2s}^k} \phi_i''(x)\phi_j''(x)\,\mathrm{d}x, & i,j = 2,3,5,6, \\ 0 & \text{for other cases,} \end{cases}$$

$$B_{1b} = [b_i]_{6\times 1} = \rho_b A_b \begin{cases} \int_0^{L_b} \phi_i(x)\,\mathrm{d}x \cdot s & (i = 1,4) \\ \int_0^{L_b} \phi_i(x)\,\mathrm{d}x \cdot c & (i = 2,3,5,6), \end{cases} \qquad B_{2b} = \frac{\dot{B}_{1b}}{\dot{\theta}},$$

$$B_{1r}^k = [b_i]_{6\times 1} = \rho_r A_r^k \begin{cases} \int_{x_{1r}^k}^{x_{2r}^k} \phi_i(x)\,\mathrm{d}x \cdot s & (i = 1,4), \\ \int_{x_{1r}^k}^{x_{2r}^k} \phi_i(x)\,\mathrm{d}x \cdot c & (i = 2,3,5,6), \end{cases} \quad (r = a, s), \qquad B_{2r}^k = \frac{\dot{B}_{1r}^k}{\dot{\theta}},$$

$$B_3 = \{m_L c, \ -m_L s, 0, m_R c, \ -m_R s, 0\}^{\mathrm{T}}, \qquad B_4 = -\frac{\dot{B}_3}{\dot{\theta}},$$

$$D_{1b} = [d_1]_{6\times 1} = \rho_b A_b \begin{cases} \int_0^{L_b} x\phi_i(x)\,\mathrm{d}x & (i = 1, 4), \\ 0 & (i = 2, 3, 5, 6), \end{cases}$$

$$D_{2b} = [d_i]_{6\times 1} = \rho_b A_b \begin{cases} \int_0^{L_b} x\phi_i(x)\,\mathrm{d}x & (i = 2, 3, 5, 6), \\ 0 & (i = 1, 4), \end{cases}$$

$$D_{3b} = [d_1]_{6\times 1} = \rho_b A_b \begin{cases} \int_0^{L_b} \phi_i'(x)\,\mathrm{d}x & (i = 2, 3, 5, 6), \\ 0 & (i = 1, 4), \end{cases}$$

$$D_{1r}^k = [d_i]_{6\times 1} = \rho_r^k A_r^k \begin{cases} \int_{x_{1r}^k}^{x_{2r}^k} x\phi_i(x)\,\mathrm{d}x & (i = 1, 4), \\ 0 & (i = 2, 3, 5, 6), \end{cases} \quad (r = a, s),$$

$$D_{2r}^k = [d_1]_{6\times 1} = \rho_r^k A_r^k \begin{cases} \int_{x_{1r}^k}^{x_{2r}^k} x\phi_i(x)\,\mathrm{d}x & (i = 2, 3, 5, 6), \\ 0 & (i = 1, 4), \end{cases} \quad (r = a, s),$$

$$D_{3r}^k = [d_i]_{6\times 1} = \rho_r^k I_r^k \begin{cases} \int_{x_{1r}^k}^{x_{2r}^k} \phi_i'(x)\,\mathrm{d}x & (i = 2, 3, 5, 6), \\ 0 & (i = 1, 4), \end{cases} \quad (r = a, s),$$

$D_4 = \{0, 0, I_L, 0, m_R, L_b, I_R\}^{\mathrm{T}}$, $\quad D_5 = \{0, 0, 0, m_R L_b, 0, 0\}^{\mathrm{T}}$,
In all the above equations, $c = \cos\theta$, $s = \sin\theta$.
In equation (14),

$$G_a = diag\left(\frac{\xi_{33}^{\mathrm{T}} A_a^1 L_a^1}{h_a^{1^2}}, \frac{\xi_{33}^{\mathrm{T}} A_a^2 L_a^2}{h_a^{2^2}}, \ldots, \frac{\xi_{33}^{\mathrm{T}} A_a^{n_a} L_a^{n_a}}{h_a^{n_a^2}}\right),$$

and in equation (10),

$$d_s = [d_{ij}]_{n_s\times 6} = \begin{cases} \dfrac{e_{31}^s h_s^i}{(\xi_{33}^{\mathrm{T}} - d_{31}^s E_s) L_s^i} \displaystyle\int_{x_{1s}^i}^{x_{2s}^i} \phi_j' & \text{(The upper and lower layers of the } i\text{th sensor are polarized in the same direction, and } j = 1, 4.) \\ \dfrac{e_{31}^s h_s^i (y_{1s}^i + y_{2s}^i)}{2(\xi_{33}^{\mathrm{T}} - d_{31}^s E_s) L_s^i} \displaystyle\int_{x_{1s}^i}^{x_{2s}^i} \phi_j''(x)\,\mathrm{d}x & \text{(The upper and lower layers of the } i\text{th actuator are polarized in reverse directions, and } j = 2, 3, 5, 6.) \\ 0 & \text{(For other cases.)} \end{cases}$$